

Geophysical Research Letters

RESEARCH LETTER

10.1029/2020GL089257

Key Points:

We present the first application of an alkenone isomer-based RIK_{37} index as salinity proxy in Lake Sayram. Lake water freshened abruptly since the early Little Ice Age. Wet conditions during CE 1150 and 1850 to present may be related to Arctic sea ice expansion and anthropogenically induced warming.

Supporting Information:

- Supporting Information S1
- Supporting Information S2

Correspondence to:
 Y. Yao and J. Lan,
 yao yuan@xjtu.edu.cn;
 lanjh@irecas.cn

Citation:
 Yao, Y., Lan, J., Zhao, J., Vachula, R.S., Xu, H., Cai, Y., et al. (2020) Abrupt freshening since the early Little Ice Age in Lake Sayram of arid central Asia inferred from an alkenone isomer proxy. *Geophysical Research Letters*, 47, e2020GL089257. <https://doi.org/10.1029/2020GL089257>

Received 9 JUN 2020
 Accepted 31 JUL 2020
 Accepted article online 6 AUG 2020

Abrupt Freshening Since the Early Little Ice Age in Lake Sayram of Arid Central Asia Inferred From an Alkenone Isomer Proxy

Yuan Yao^{1,2}  , Jianghu Lan^{2,3}  , Jiaju Zhao²  , Richard S. Vachula⁴  , Hai Xu⁵  , Yanjun Cai¹  , Hai Cheng¹  , and Yongsong Huang^{4,2} 

¹Institute of Global Environmental Change, Xi'an Jiaotong University, Xi'an, China, ²State Key Laboratory of Loess and Quaternary Geology, Institute of Earth Environment, Chinese Academy of Sciences, Xi'an, China, ³Center for Excellence in Quaternary Science and Global Change, Chinese Academy of Sciences, Xi'an, China, ⁴Department of Earth, Environmental and Planetary Sciences, Brown University, Providence, RI, USA, ⁵Institute of Surface-Earth System Science, Tianjin University, Tianjin, China

Abstract Hydroclimatic variations of arid central Asia (ACA) significantly impact regional ecosystems and human civilizations. Here we present a lake water salinity record of the last 3,000 years from Lake Sayram in the core area of ACA using a new alkenone isomer-based RIK_{37} index. Our record shows an abrupt decrease in salinity by more than 5‰ since the "early" Little Ice Age (LIA) (about CE 1150), which can be attributed to the combined effect of regional wetting, cooling, and topographic features. Combined with other moisture records in the region, we find two periods of relatively wet conditions during CE 1150-1550 and 1850 to present, which maybe linked to Arctic sea ice expansion due to natural variability and, from CE 1950, anthropogenically induced warming. The wet conditions during CE 1206-1260 may have favored the spread of the Mongol Empire across the entire core area of ACA.

Plain Language Summary Arid central Asia (ACA), one of the largest arid zones in the world, suffers from water resource scarcity, which impacts the regional ecosystems and human civilizations. Reconstructions of lake water salinity in ACA can provide valuable information on past overall hydroclimatic changes, which is of crucial importance for our understanding of past and future climates. Here we apply a new salinity proxy, based on the lipid biomarkers of haptophyte algae, to quantitatively reconstruct salinity changes of the last 3,000 years from Lake Sayram in the core area of ACA and find an abrupt freshening of lake water since the early Little Ice Age (LIA). Our reconstruction, together with other moisture records in the region, indicate relatively wet conditions at two intervals during CE 1150-1550 and 1850 to present, which are associated with natural and anthropogenic forcing. During the period of CE 1206-1260, the favorable wet conditions may have aided the spread of the Mongol Empire across the entire core area of ACA.

1. Introduction

Arid central Asia (ACA), one of the largest arid zones in the world, extends across the midlatitude Asian continent from the Caspian Sea in the west to the boundary of the modern Asian summer monsoon in the east (Figure 1a). Its present climate, especially in the core area (central and western region) of ACA, is primarily regulated by westerly circulation (Chen et al., 2019). The region suffers from water resource scarcity, which significantly impacts regional ecosystems and human civilizations (e.g., Putnam et al., 2016). In the past few decades, numerous instrumental data have demonstrated that the regional climate has gradually become wetter as the global climate warms (Chen et al., 2011; Shi et al., 2007; Yao et al., 2020). Hydrological reconstructions of the past two millennia in the region can provide insights regarding the natural background level of variability and hydrological process in response to human-nature interactions, which are of crucial importance for understanding the mechanisms of hydroclimatic changes.

Numerous studies have reconstructed the hydroclimatic changes of the core area of ACA over different time scales from various geological archives, such as lake sediments (e.g., Chen et al., 2008; Lan et al., 2018, 2019, 2020; Rudaya et al., 2009; Wang & Feng, 2013), stalagmites (e.g., Cai et al., 2017; Chen et al., 2012, 2016), loess deposits (e.g., Chen et al., 2016; Ran & Feng, 2014), and peats (Hong et al., 2014; Xu et al., 2019). Most of

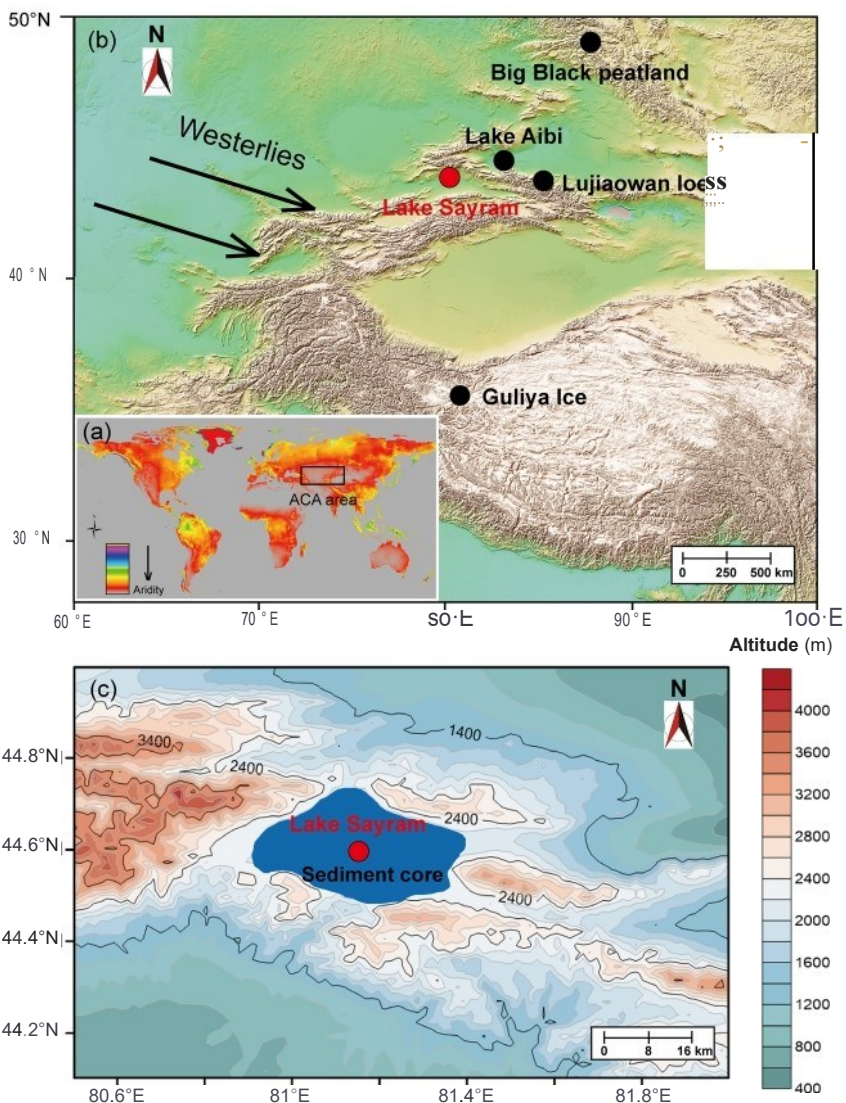


Figure 1. (a) Global aridity map and location of arid central Asia (ACA) (Dataset of Global Aridity Index is from the CGIAR-CSI GeoPortal (<http://www.cgiar.org>); Trabucco & Zomer, 2009). (b) Location of different records on a topographic map. Geographic information data are from CGIAR Consortium for Spatial Information (CGIAR-CSI), <http://srtm.cgiar.org/SELECTION/inputCoord.asp>. (c) Contour map showing the location of Lake Sayram sediment core and the surrounding geographic information.

these studies focused on effective moisture changes during the Holocene or longer time scales; the moisture evolution of the past two millennia and its driving mechanisms in the region, however, are still poorly understood, largely due to influence of the nonmoisture factors on the proxies employed and/or relatively large age uncertainties on such short time scales. For example, temperature played the predominant role over moisture in controlling the variations of high-resolution speleothem ^{18}O in Kesang Cave during the past two millennia (Cai et al., 2017). Loess-paleosol sequences have low temporal resolution and relatively large age errors on short time scales (Chen et al., 2016).

Recent studies have proposed that the RIK₃₇ index based on the isomeric ratio of tri-unsaturated C₃₇ alkenones can be used as a salinity proxy in freshwater/oligohaline environments for past hydrological reconstructions (Kaiser et al., 2019; Longo et al., 2016). Long-chain alkenones (LCAs) are a class of C₃₅-C₄₂ di-, tri-, and tetra-unsaturated methyl (Me) and ethyl (Et) ketones, exclusively produced by certain Isochrysidales within haptophyte lineages. In lacustrine settings, there are obvious transitions of two alkenone-producing Isochrysidales groups as salinity increases (Longo et al., 2016): Group I occurs in

freshwater/oligohaline lakes (Longo et al., 2016, 2018; Y. Yao et al., 2019), whereas Group II occurs in oligohaline/saline lakes, and its relative abundances increase with increasing salinity (Longo et al., 2016; Theroux et al., 2010). The distinctive LCA distributions of Group I Isochrysidales are characterized by the presence of isomeric tri-unsaturated C₃₇ alkenones with $\text{I}_1^{14,21,28}$ double bond positions (C_{37,9}), in addition to the common $\text{I}_1^{7,14,21}$ (C_{37,8}) in Group II. Given the differences in LCA distributions and salinity tolerance of Groups I and II Isochrysidales, the **RIK₃₇** thus can be applied as an indicator of salinity changes in freshwater/oligohaline environments (Kaiser et al., 2019).

LakeSayram in western ACA is currently an oligohaline alpine lake (measured salinity: 1.62‰ in summer of 2017) and contains mixed Groups I and II LCAs in surface sediments (Song et al., 2016). Here, we present an ~3 ka long, multidecadal resolution hydroclimatic record based on the **RIK₃₇** salinity proxy from Lake Sayram. Our study verifies the application of the **RIK₃₇** proxy for quantitative paleosalinity reconstruction in lakes and shows relatively wet conditions at two intervals between CE 1150- 1550 and 1850 to present since the early Little Ice Age (LIA) associated with westerly circulation and warming-induced local atmospheric water cycling.

2. Material and Methods

2.1. Study Site

LakeSayram (44°30' to 44°42'N, 81°05' to 81°15'E; 2,074 m a.s.l.; Figures 1b and 1e), located in the Central Tianshan Mountains (northern slope) of northwestern China (Xinjiang region), is a hydrologically closed terminal alpine lake. The lake has an area of ~462 km² with a maximum water depth of ~99 m and a mean depth of ~56 m and is surrounded by the Keguqin, Kusunmuqieke, Hanziga, and Shaliqieke mountains. The lake water is supplied mainly by several rivers from the west and northwest, and the river water derives from rainfall, groundwater, and melting snow from the surrounding mountains. Due to the limited glacier extent (4.28 km²) on the surrounding mountains, glaciers provide little water supply to the rivers during the warm seasons (Lan et al., 2019). In recent decades, the annual water inflow into Lake Sayram is ~2.524 x 10⁸ m³, which is in equilibrium with annual lake water evaporation (~2.492 x 10⁸ m³) (S. Wang & Dou, 1998). The regional mean annual air temperature was ~3.9°C, and the mean annual precipitation was ~236 mm between CE 1958 and 2016, with a maximum in summer and minimum in winter (Lan et al., 2019).

2.2. Sediment Core and Dating

A 98 cm sediment core (SLM13-2-2) was retrieved from the center of Lake Sayram at a water depth of 83 m in August 2013, using a 60-mm UWITEC gravity corer (Figure 1e). It was very close to another parallel sediment core (SLM13-2-1; Lan et al., 2019, 2020) within an area of ~1 m². The core was subsampled at 1 cm intervals. All collected samples were kept in a cooler with gel ice packs in the field and then frozen at ~20°C in the laboratory until analysis. The age profile of another parallel sediment core (SLM13-2-1) has been well established by ¹³⁷Cs-²¹⁰Pb dating and a ¹⁴C model (Lan et al., 2019, 2020). Bulk carbonate contents in our sediment core were determined by titration with diluted perchloric acid (HClO₄; 0.1 mol·L⁻¹) for comparison with previously published values in another core (SLM13-2-1; Table S1 in the supporting information; Lan et al., 2019). By stratigraphically correlating the carbonate content peaks of the two cores, the chronology in our core was established by using linear interpolation (Figure S1). The general correspondences of the carbonate content peaks confirm the reliability of the chronology.

2.3. LCA Analysis

All samples were freeze-dried and extracted by sonication (3X) with dichloromethane (DCM)/methanol (MeOH) (9:1, v/v). The extracts were purified by column chromatography with silica gel using n-hexane and DCM, respectively. The DCM fractions were further purified by column chromatography with silver thiolate silica (Aponte et al., 2013; L. Wang, Longo, et al., 2019). An increasing polarity sequence of solvents (hexane: DCM [2 ml, 2:1, v:v], DCM [1 ml], and acetone [2 ml]) was used to separate compounds. All LCAs were retained in the acetone fractions (L. Wang, Longo, et al., 2019; Zheng et al., 2017). LCAs were then analyzed by an Agilent 7890N GC system equipped with a flame ionization detector (FID) and a Restek Rtx-200 GC column (105 m x 250 μm x 0.25 μm). The following GC-FID oven program was used: initial temperature of 50°C (hold 2 min), ramp 20°C/min to 255°C, and ramp 3°C/min to 320°C (hold 25 min). LCA peak

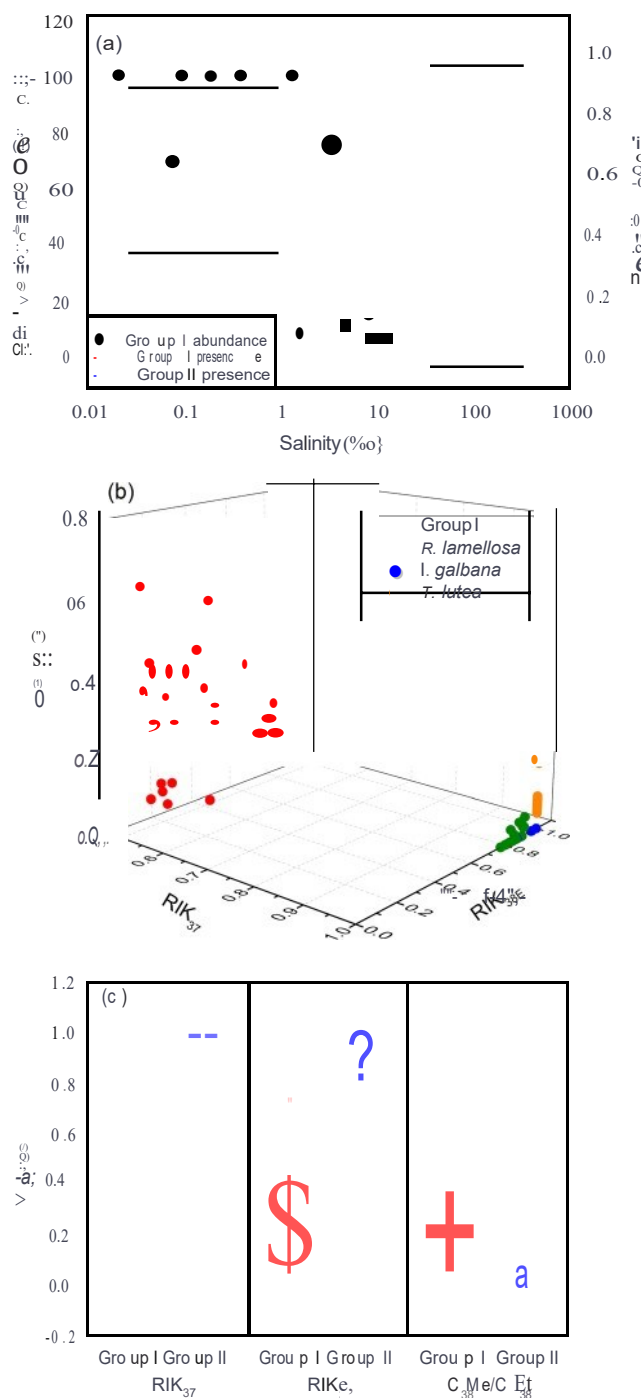


Figure 2. (a) Abundance of Group I Isochrysidales (relative to Group II) versus salinity and logistic probability for the presence of Group I and II Isochrysidales (Isochrysidales DNA data of lakes are from Araie et al., 2018; D'Andrea et al., 2016; Kaiser et al., 2019; Plancq et al., 2018, 2019; Richter et al., 2019; Theroux et al., 2010; K. J. Wang, O'Donnell, et al., 2019; Y. Yao et al., 2019; Table S2). (b) Three-dimensional diagram showing the published LCA indices (RIK₃₇, RIK_{38E}, and C₃₈Me/C₃₈Et) between Groups I (Longo et al., 2016, 2018; K. J. Wang, O'Donnell, et al., 2019; Y. Yao et al., 2019) and II (*R. lamellosa*, *I. galbana*, and *T. lutea*; Zheng et al., 2019). (c) Box plot showing the range and median values of the published RIK₃₇, RIK_{38E}, and C₃₈Me/C₃₈Et of Group I and II.

identification was accomplished by comparison of retention times with the Greenland surfacesediments (Longo et al., 2013) as an alkenone standard.

Group I Isochrysidales feature the presence of isomeric tri-unsaturated C₃₁ (C₃₁:3b) and C₃₈Et (C₃₈:3bEt) alkenones as well as C₃₈Me, whereas Group II Isochrysidales almost do not produce these compounds (Longo et al., 2016; Zheng et al., 2019). Thus, the following indices were calculated using the peak area of the individual LCAs and were used to estimate the occurrence of Group I Isochrysidales in our sediment core (Kaiser et al., 2019; Longo et al., 2016):

$$RIK_{37} = \frac{[C_{37}:3a]}{[C_{37}:3a + C_{37}:3b]} \quad (1)$$

$$RIK_{38E} = \frac{[C_{38}:3aEt]}{[C_{38}:3aEt + C_{38}:3bEt]} \quad (2)$$

$$C_{38}Me/C_{38}Et = \frac{[C_{38}Me]}{[C_{38}Et]} \quad (3)$$

where the "a" and "b" subscripts refer to the t_{7.14} and t_{21.28} tri-unsaturated LCAs, respectively.

2.4. Statistical Analyses

Logistic regression was applied using MATIAB to published DNA data of Groups I and II Isochrysidales to determine the likelihood of the presence of Groups I and II Isochrysidales along a salinity gradient.

3. Results and Discussion

3.1. LCA-Based Salinity Proxies in Freshwater/Oligohaline Lakes

We reviewed the published DNA data of Groups I and II Isochrysidales from globally distributed lakes and the Bothnian Bay in the Baltic Sea (Figure 2a and Table S2; Araie et al., 2018; D'Andrea et al., 2016; Kaiser et al., 2019; Plancq et al., 2018, 2019; Richter et al., 2019; Theroux et al., 2010; K. J. Wang, O'Donnell, et al., 2019; Y. Yao et al., 2019) and determined their probability of presence along a salinity gradient using logistic regression (Figure 2a and Table S2). Our statistical analyses do not contain the DNA data from the downstream Baltic Sea (Bothnian Sea, Landsort Deep, Eastern Gotland Basin, and Arkona Basin) due to the potential inputs of Group I Isochrysidales DNA from upstream Bothnian (Kaiser et al., 2019). Our analyses show that Group I Isochrysidales typically occur in freshwater lakes (salinity: <~1‰) with very high likelihood (0.87) of presence, whereas Group II Isochrysidales predominantly occur in saline to hyperhaline lakes (salinity: >~10‰) with the presence likelihood of ~1, which is in agreement with the salinity tolerance of Groups I and II Isochrysidales that was first proposed by Longo et al. (2016). Note that there is the occurrence of small numbers of Group II Isochrysidales in some freshwater lakes under certain specific environmental conditions (Figure 2a and Table S2), which was first found by Y. Yao et al. (2019) in two

anthropogenically impacted freshwater volcanic lakes of northeastern China and was subsequently observed in freshwater North Killeak of Alaska (K. J. Wang, O'Donne ll, et al., 2019). Importan tly, both Groups I and II thrive in oligohaline lakes (salinity: - 1-11‰), and Group II appears to become increasingly more competitive against Group I as salinity increases. Such transitions may be related to the different requirements of certain major ions and /or nutrients for Group I and II Isochrysidales. Group I preferentially thrives in the oligotrophic freshwater environments with reduced major ions (Y. Yao et al., 2019), whereas Group II appears to have morestringent requirements for common major ions, such as Ca^{2+} , Mg^{2+} , and Na^+ (Pearson et al., 2008). As salinity increaseswith increasesof certain major ions, Group II might gradually outcompete Group I.

We compiled the published RIK_{37} , RIK_{38E} , and $\text{C}_{38}\text{Me/C}_{38}\text{Et}$ of Groups I and II LCAs (Table S3; Longo et al., 2016, 2018; K. J. Wang, O'Donnell, et al., 2019; Y. Yao et al., 2019; Zheng et al., 2019). Group II LCA data are from culture experiments of three common Group II species, *Isochrysis galbana*, *Ruttnera (Chrysotila) lamellosa*, and *Tisochrysis lutea* (Zheng et al., 2019). However, so far, there have been no studies successfully isolating and cultur ing the Group I Isochrysidales, so the surfacesediments of freshwater lakes with Group I-type LCA distributions were used for Group I (Longo et al., 2016, 2018; K.J. Wang , O'Donnell, et al., 2019; Y. Yao et al., 2019). The three-dimensional diagram showing our compiled RIK_{37} , RIK_{38E} , and $\text{C}_{38}\text{Me/C}_{38}\text{Et}$ values clearly different iat es the Group I LCA distribut ions from the Group II LCAs (Figure 2b). Group I LCAs have lower RIK_{37} (0.56 ± 0.03) and RIK_{38E} (0.22 ± 0.12) values as well as higher $\text{C}_{38}\text{Me/C}_{38}\text{Et}$ (0.31 ± 0.13) relative to Group II LCAs (RIK_{37} : 1; RIK_{38E} : 0.96 ± 0.06 ; $\text{C}_{38}\text{Me/C}_{38}\text{Et}$: 0.03 ± 0.0036) (Figure 2c). Based on the above rationale, the RIK_{37} (Kaiser et al., 2019; Longo et al., 2016) as well as potent al RIK_{38E} and $\text{C}_{38}\text{Me/C}_{38}\text{Et}$ can be applied as indicators of sa linity changes in freshwater/oligohaline environments. However, there is more scatter of RIK_{38E} and $\text{C}_{38}\text{Me/C}_{38}\text{Et}$ for Groups I and II LCAs relative to RIK_{37} (F igure 2c), indicating thatother environmental factors, suchas temperature(Longo et al., 2016), and relatively tiny production of $\text{C}_{38,31}\text{Et}$ and C_{38}Me in Group II mayalso affect the RIK_{38E} and/or $\text{C}_{38}\text{Me/C}_{38}\text{Et}$ values. We suggest, therefore, that RIK_{37} may a better salinity proxy for paleohydrological reconstructions.

3.2. Reconst ruction of Salinity Changes Using the Lake Sayram Sediment Core

Our sediment core from Lake Sayram displays two typical LCA profiles: mixed Group 1/11 and Group II (Figure S2). Mixed Group 1/11 LCAs are characterized by the presence of $\text{C}_{37,3b}$, $\text{C}_{38,3b}\text{Et}$, and C_{38}Me (Figure S2a), whereas Group II LCAs genera lly do not conta in these compounds (Figure S2b). Before about CE 1100, the RIK_{37} remains at the constant value of 1 (Figure S3a), indicating a dominance of Group II Isochrysidales, which is further verified by the constant RIK_{38E} and $\text{C}_{38}\text{Me/C}_{38}\text{Et}$ valuesof 1 and 0, respectively (FiguresS3d and S3e). After about CE 1100, the RIK_{37} shows an abrupt decrease(1-0.67) from about CE1100 to 1200, followedby the relatively small fluctuations between 0.65and 0.79 to present (Figure S3a), indicating a transition from Group II to mixed Group1/11. S im ilar ly, the var i ations in RIK_{38E} and $\text{C}_{38}\text{Me/C}_{38}\text{Et}$ also indicate such a transition of Isochrysidales groups at that time(FiguresS3d and S3e).

We quantitatively estimate the changes in relative contribution of Group I LCAs in our sediment core using an end member mixing approach (Longo et al., 2018; Table S4).

$$\text{Group I} = \frac{\text{RIK}_{37}-\text{sample} - \text{RIK}_{37}-\text{group II}}{\text{RIK}_{37}-\text{group I} - \text{RIK}_{37}-\text{group II}} \times 100$$

whereGroup I is the fract ion of Group I LCAs in sed iments (%). RIK_{37} -sample is the RIK_{37} values in a given sediment sample. RIK_{37} -Group I is the end member value (0.56 ± 0.028 ; Longo et al., 2018) of RIK_{37} for Group I. RIK_{37} - group II is the end member value (1; Longo et al., 2018) of RIK_{37} for Group II.

Our resultsshow that Group I LCAs do not contr ibute to the sedimentary LCA pool before CE1100, whereas the contribution increases to $67\% \pm 7\%$ after CE 1100 (Figure S3b and Table S4).Such increasesin Group I LCA contr ibutions indicate freshen ing of lake water at that time favorable for the growth of Group I Isochrysidales. Employing the published RIK_{37} -salinity calibration (salin ity = $14.77 \times \text{RIK}_{37} - 7.86$; root mean square error (RMSE): - 1. 2‰; Kaiser et al., 2019), we quant itatively reconstruct the salinity changes in Lake Sayram during the last ~3,000 years (Figure S3c and Table S4). Note that this calibration is the

onlyone available at present, but further studies on regional calibration would help improve the accuracy of the reconstructed salinity. Before about CE1100, our reconstructed salinity is more than -7\%o . Note that the RIK_{37} valueof 1 reaches the threshold as a salinity proxy, because Group II Isochrysidalesbecome the dominant Isochrysidalesgroup when salinity exceeds the threshold of -7\%o based on the calibration from Kaiser et al. (2019). After about CE1100, the salinity abruptly decreases by more than 5\%o from about CE1100 to 1200 and continues to maintain oligohaline environments, with the small fluctuations of salinity ($2.5\text{\%o} \pm 0.5\text{\%o}$), until the present. The abrupt freshening of lake water starting from about CE 1100 to 1200 is coeval with the onset of the early LIA (about CE 1150; Barclay et al., 2009; Luckman, 2000).

3.3. Two Periods of Relatively Wet Conditions in ACA Since the Early LIA

Our reconstructed salinityshows an abrupt fresheningin LakeSayramssincethe early LIA, indicating a positive hydrological balance. Due to the limited glacier extent (4.28 km^2) on the surrounding mountains, ice/snow meltwater has a negligible impact on changes in lake water salinity (Lan et al., 2019). The timing of the abruptfreshening in our record is coeval with the rapid regional cooling and wetting inferred from tree ring index of Western Central Asia (Esper et al., 2002) and 5^{18}O and 5^{13}C values of bulk carbonate in Lake Sayram (Lan et al., 2020), respectively (Figures 3c- 3e),suggesting the impacts of cooling and wetting on the positive water balance. Moreover, regional topographic features of LakeSayram may also play an important role in controlling the moisture patterns. Lake Sayram is located at the northern slope of the Tianshan Mountain with high altitude, where the dominant water source from northerly and northwesterly winds can be largely condensed into orographic rainfall (S. Wang et al., 2017). Therefore , such large decreases in lake water salinity (by more than 5\%o) may result from the combined effect of regional cooling, wetting, and topographic features.

Our salinity record displays relative freshening of lake water at two intervals of about CE 1150-1550 and 1850 to present since the early LIA, which is consistent with the effective moisture records of the published 5^{18}O and 5^{13}C valuesof bulk carbonate in Lake Sayram (Lan et al., 2020) (Figures 3d and 3e).The relatively wet periods appear to be recorded broadly in other moisture records in the core area of ACA, including *Artemisia* and *Chenopodiaceae* pollen ratio (A/C ratio) in Lake Aibi (W. Wang & Feng, 2013), A/C ratio and 5^{13}C values of cellulose in Big Black peatland (Xu et al., 2019), magnetic properties (Chen et al., 2016) and 5^{13}C values of bulk organic matter (Xie et al., 2018) in Lujiaowan loess, and accumulation of the Guliya ice core on the northwestern Tibetan Plateau (T. Yao et al.,1996)(Figures 3f- 3i).The timing and rate of wetting shows some differences among these records, possibly due to dating uncertainties, different sensitivities of the proxies for moisture changes, and/or local moisture circulation in different topographic settings. For example, the Lujiaowan loess (Chen et al., 2016; Xie et al., 2018) and Lake Aibi (W. Wang & Feng, 2013) records may have relatively large age errors on short time scales based on quartz OSL and K-feldspar pIRIR dating and limited ^{14}C age data, respectively. The pollen A/C ratio in arid and semiarid regions, especially in the saline-alkali area surrounding Lake Aibi (hypersaline lake; salinity: 112\%o ; Song et al., 2016), in response to moisture changes also depends on regional *Artemisia* and *Chenopodiaceae* biomass, with low sensitivity under the low biomass conditions (W. Wang & Feng, 2013). Tianshan Mountain serves as a barrier to significantly affect the transport of northerly and northwesterly moisture toward the Tibetan Plateau and causes more precipitation at the northern slope of the Tianshan Mountain (S. Wang et al., 2017), which may be an important factor leading to our observed difference in the timing of relatively wet conditions between our record and the Guliya ice core.

3.4. Control of the Westerlies and Warming on HydrologicalChanges

Based on modern meteorology and isotopic tracing of hydrology, numerous studies have demonstrated that thewesterlies are the dominant moisture transport drivers in ACA(e.g., Aizen et al.,2006;Huang et al., 2015; Liu et al., 2009; S.Wang et al., 2017). Especially, Huang et al.(2015)and Chen et al. (2019) recently proposed a core area of ACA,where the climate is considered to be primarily regulated by the westerly circulation on annual, decadal, and longer time scales. However, some studies suggested that the Asian Summer Monsoon (ASM) and /or Indian Summer Monsoon (ISM) might reach at leastwestern ACA as important water vapor sources during the early and/or middle Holocene (e.g., Cheng et al., 2012; Harrison et al., 1996; Ricketts et al., 2001; Rudaya et al., 2009). The hydrological pattern of the past 2,000 years in our record is not associated with variabilities in ASM and ISM as indicated by the speleothem 5^{18}O values of Wangxiang Cave

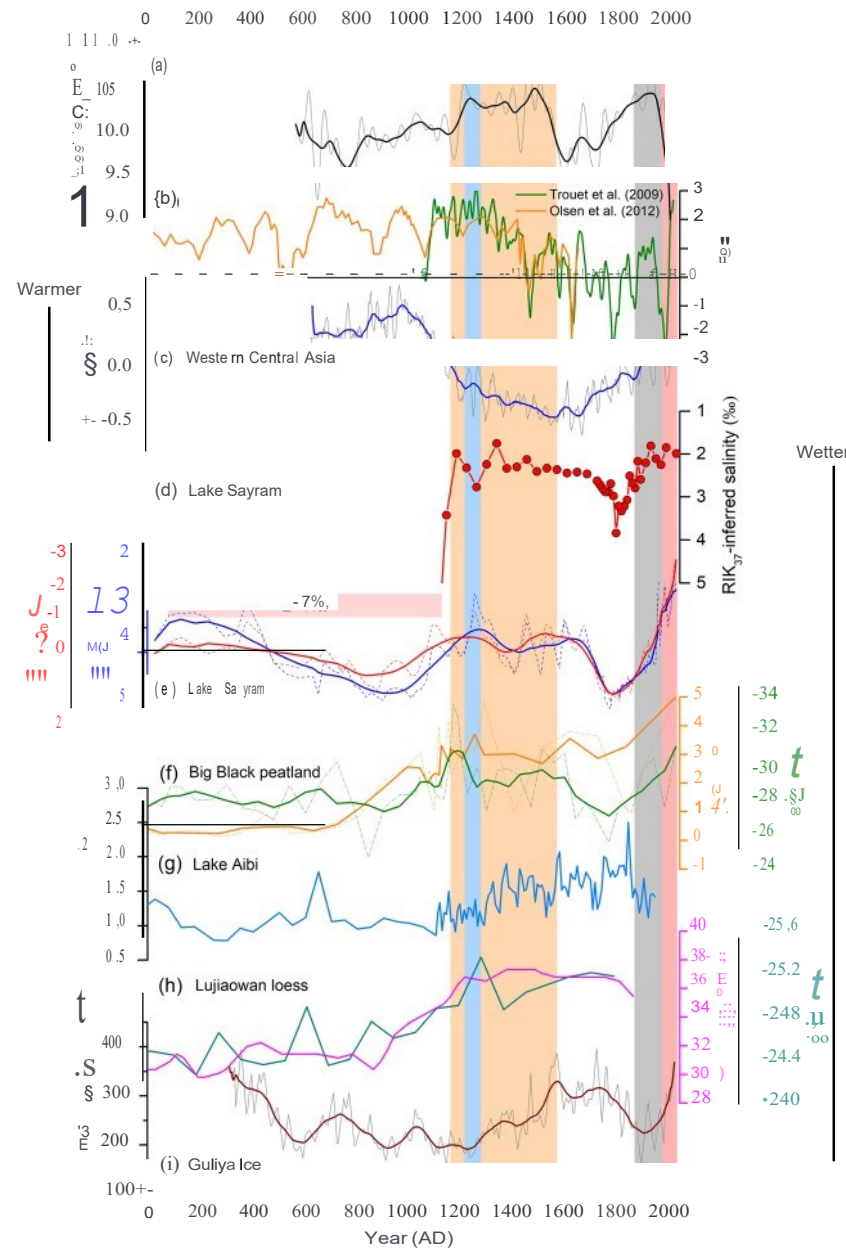


Figure 3. Comparison of RIK₃ inferred salinity in Lake Sayram downcore of the past 2000 years with other records. (a) Arctic sea ice extent reconstructed from a series of terrestrial proxies in the circum-Arctic region (Kinnard et al., 2011; black line represents 100-point running means). (b) NAO index inferred from Morocco tree ring and Scotland speleothem (Trouet et al., 2009) and southwest Greenland lake sediments (Olsen et al., 2012). (c) The regional temperature record of tree ring index from Western Central Asia (Esper et al., 2002; blue line represents 20-point running means). (d) RIK₃ inferred salinity in Lake Sayram downcore. (e) $\delta^{13}\text{C}$ and $\delta^{18}\text{O}$ values of bulk carbonate in Lake Sayram (Lan et al., 2020; red and blue lines represent 10-point running means). (f) pollen A/C ratio and $\delta^{13}\text{C}$ values of cellulose in Big Black peatland (Xu et al., 2019; orange line represents 3-point running means for $\delta^{13}\text{C}$ ratio, green line represents 5-point running means for $\delta^{13}\text{C}$ values). (g) A/C ratio in Lake Aibi (W. Wang & Feng, 2013). (h) $\delta^{13}\text{C}$ values of bulk organic matter (Xie et al., 2018) and magnetic index CxAiw/SIRM; Chen et al. (2016) in Lujiaowan loess profile (LJW10), Yili valley. (i) Accumulation of Guliya Ice (T. Yao et al., 1996; crimson line represents 20-point running means). Orange shaded area represents the age from 1150 to 1550; gray shaded area represents the age from 1850 to 1950; red shaded area represents the age from 1950 to 2010; light blue shaded area represents the age from 1206 to 1260 that is duration of the Mongol Empire expansion.

(Zhang et al., 2008) and composites of Jhumar and Wah Shikar Caves (Sinha et al., 2011), respectively (Figure S4). We propose, therefore, that the westerly circulation is major driving factor of the hydrological pattern of the past 2,000 years in the core area of ACA under natural climatic conditions.

The intensity of the westerlies and the location of the westerlyjet may play an important role in controlling the overall rainfall pattern in the core area of ACA on multicentennial and millennium time scales (Chen et al., 2019). The larger meridional thermal gradient between high and middle latitudes and the negative phase of North Atlantic Oscillation (NAO), as two potential driving factors, can directly or indirectly lead to a strengthening of westerly winds and southward movement of the westerly jet (e.g., Chen et al., 2019; Lan et al., 2020). This can bring more water vapor supply from the major water bodies (Mediterranean Sea, Black Sea, and Caspian Sea, even North Atlantic)(Jin et al., 2012; S. Wang et al., 2017) to the core area of ACA along the westerly pathways. We compared our record, together with the published $\delta^{18}\text{O}$ and $\delta^{13}\text{C}$ data of bulk carbonate (Lan et al., 2020), with proxy-based reconstructions of summer Arctic sea ice extents (Kinnard et al., 2011) and an NAO index (Olsen et al., 2012; Trouet et al., 2009)(Figures 3a, 3b, 3d, and 3e). During about CE1150-1550 and 1850-1950, the abrupt and/or persistent wetting conditions coincided with the expansion of Arctic sea ice that leads to larger meridional thermal gradients (Coulomou et al., 2018), but the NAO was mainly in its positive phase. This indicates that Arctic sea ice expansion, rather than the NAO, may have played a critical role in driving the wet climate at that time. Indeed, observational data of the recent few decades display that the NAO does not exercise a significant control on the mean annual precipitation of our study region (Figure S5). However, from about CE 1950 to present, Arctic sea ice rapidly retreated and the NAO shifted toward the positive phase. The persistent moisture conditions since CE 1950 may be associated with the enlanced local atmospheric water cycle with the anthropogenically induced accelerated warming (J. Yao et al., 2020). We thus suggest that the core area of ACA, at least the Xinjiang region, would experience relatively wet conditions under anticipated global warming for a certain period of time in the future. Together, the two relatively wet periods since the early LIA likely resulted from natural variations of the larger meridional thermal gradient primarily driven by Arctic sea ice expansion and anthropogenic warming-induced enhancement of the local atmospheric water cycle.

3.5. Relatively Wet Conditions in ACA and the Expansion of the Mongol Empire

The Mongol Empire, the largest contiguous land empire in the history of the world, rapidly expanded from CE1206 to 1260, with its largest areal extent in CE 1241 stretching from China to Europe across the core area of ACA (Putnam et al., 2016). Pederson et al. (2014) presented a 15-year episode of persistent moisture (CE 1211- 1225) in central Mongolia based on a tree ring record and suggested that such wet conditions favored the Mongol rise. The wetter-than-present conditions in the Tarim Basin of interior Asian deserts since the early LIA (from CE1180 to present), as inferred from geomorphic and chronologic evidences, are suggested to have aided the spread of the Mongol Empire across the deserts (Putnam et al., 2016). However, the -800-year record in the Tarim Basin did not show how moisture changed before the early LIA (or onset of Mongol rise: CE 1206). Our record of the past 2000 years extends beyond the early LIA and indicates a pronounced wetting in the broader core area of ACA after the early LIA, together with comparison of other published moisture records in the region (Figures 3d- 3i). This provides more convincing evidence for the role of wet conditions in the spread of the Mongol Empire across the entire core area of ACA.

Grassland was the most important source of energy exploited by the Mongol Empire. The consistently wet conditions would have led to flourishing grassland biomass (Zhao et al., 2019), which would have fueled the horses upon which the military conquests of the Mongol Empire mainly depended (Pederson et al., 2014; Putnam et al., 2016). Moreover, the grass could also be efficiently converted to other energy (e.g., meat and milk) for the food supply of the Mongol Empire soldiers. The timing of abrupt wetting in the core area of ACA since the early LIA is generally coeval with onset of the Mongol rise (CE1206) (Figures 3d- 3i), suggesting that such favorable wetting conditions aided Mongol conquests across Eurasia.

4. Conclusions

Our quantitative reconstruction of lake water salinity based on a new alkenone isomer proxy from alpine Lake Sayram indicates an abrupt freshening of lake water in the core area of ACA since the early LIA. The abrupt decrease in lake water salinity by more than 5‰ can be attributed to the combined effects of regional cooling, wetting, and topographic features. Together with published moisture records in the

region, these results show clear evidence of two periods of relatively wet conditions during about CE 1150-1550 and 1850 to present. This may have resulted from a strengthening of westerly winds and the southward movement of the westerly jet due to natural variability likely driven by Arctic sea ice extent, as well as increased local atmospheric water cycling under anthropogenically induced warming. We suggest, therefore, that relatively wet conditions are expected in the core area of ACA, at least in the Xinjiang region, with anticipated global warming for a certain period of time in the future. During the period of CE 1206-1260, persistently wet conditions may have significantly contributed to the spread of the Mongol Empire across the core area of ACA.

Data Availability Statement

The research data used in this study are submitted to the datasets of 4TU Centre for Research Data, which will be available at <http://doi.org/10.4121/uuid:b9d712d9-a325-4d7ab36e-ef017d88808c>. The research data also can be downloaded from the supporting information (Tables S2-S4).

Acknowledgments

This work was supported by the National Natural Science Foundation of China (No. 41702187; 41888101), the Fundamental Research Funds for the Central Universities, the Strategic Priority Research Program of Chinese Academy of Sciences (XDB40010300), and the 2nd Tibetan Plateau Scientific Expedition and Research (2019QZKK0101). We thank J. Jing for assistance during sample pretreatment and M. Ran and H. Xie for providing the ^{13}C data in Lake Aibi and ^{13}C data of bulk organic matter in Lujiaowan loess. We are also grateful for the comments from two anonymous reviewers that helped to improve the manuscript.

References

Aizen, V. B., Aizen, E. M., Joswiak, D. R., Fujita, K., Takeuchi, N., & Nikitin, S. A. (2006). Climatic and atmospheric circulation pattern variability from ice- δ ore isotope /geochronology records (Altai, Tien Shan and Tibet). *Annals of Glaciology*, 43, 4. <https://doi.org/10.3189/1n 756406781812078>

Aponte, J. C., Dillon, J. T., & Huang, Y. (2013). The unique liquid chromatographic properties of Group II transition metals for the separation of unsaturated organic compounds. *Journal of Separation Science*, 36(16), 2563-2570. <https://doi.org/10.1002/jssc.201300457>

Arai, H., Nakamura, H., Toney, J. L., Haig, H. A., Plancq, J., Shiratori, T., et al. (2018). Novel alkenone-producing strains of genus *Isochrysis* (Haptophyta) isolated from Canadian saline lakes show temperature sensitivity of alkenones and alkenoates. *Organic Geochemistry*, 121, 89-103. <https://doi.org/10.1016/j.orggeochem.2018.04.008>

Barclay, D. J., Wiles, G. C., & Calkin, P. E. (2009). Holocene glacier fluctuations in Alaska. *Quaternary Science Reviews*, 28(21-22), 2034-2048. <https://doi.org/10.1016/j.quascirev.2009.01.016>

Cai, Y., Chiang, J. C. H., Breitenbach, S. F. M., Tan, I., Cheng, H., Edwards, R. I., & An, Z. (2017). Holocene moisture changes in western China, Central Asia, inferred from stalagmites. *Quaternary Science Reviews*, 158, 18-28. <https://doi.org/10.1016/j.quascirev.2016.12.014>

Chen, F., Chen, J., Huang, W., Chen, S., Huang, X., Jin, I., et al. (2019). Westerlies-Asia and monsoonal Asia: Spatiotemporal differences in climate change and possible mechanisms on decadal to sub-orbital timescales. *Earth-Science Reviews*, 192, 337-354. <https://doi.org/10.1016/j.earscirev.2019.03.005>

Chen, F., Huang, W., Jin, L., Chen, J., & Wang, J. (2011). Spatiotemporal precipitation variations in the arid Central Asia in the context of global warming. *Science China Earth Sciences*, 54(12), 1812-1821. <https://doi.org/10.1007/s11430-011-4333-8>

Chen, F., Jia, J., Chen, J., Li, G., Zhang, X., Xie, H., et al. (2016). A persistent Holocene wetting trend in arid central Asia, with wettest conditions in the late Holocene, revealed by multi-proxy analyses of loess-paleosol sequences in Xinjiang, China. *Quaternary Science Reviews*, 146, 134-146. <https://doi.org/10.1016/j.quascirev.2016.06.002>

Chen, F., Yu, Z., Yang, M., Ito, E., Wang, S., Madsen, D. B., et al. (2008). Holocene moisture evolution in arid central Asia and its out-of-phase relationship with Asian monsoon history. *Quaternary Science Reviews*, 27(3-4), 351-364. <https://doi.org/10.1016/j.quascirev.2007.10.017>

Cheng, H., Spoil, C., Breitenbach, S. F. M., Sinha, A., Wassenburg, J. A., Jochum, K. P., et al. (2016). Climate variations of Central Asia on orbital to millennial timescales. *Scientific Reports*, 6, 36,975. <https://doi.org/10.1038/sre36975>

Cheng, H., Zhang, P., Spoil, C., Edwards, R. I., Cai, Y., Zhang, D., et al. (2012). The climatic cyclicity in semiarid-arid central Asia over the past 500,000 years. *Geophysio Research Letters*, 39, L01705. <https://doi.org/10.1029/2011gl050202>

Coumou, D., Capua, G. D., Vavrus, S., Wang, L., & Wang, S. (2018). The influence of Arctic amplification on mid-latitude summer circulation. *Nature Communications*, 9, 2959. <https://doi.org/10.1038/s41467-018-05256-8>

D'Andrea, W. J., Theroux, S., Brackley, E. S., & Huang, X. (2016). Does phylogeny control U_{C} -temperature sensitivity? Implications for lacustrine alkenone paleothermometry. *Geochimica et Cosmochimica Acta*, 175, 168-180.

Esper, J., Schweingruber, F. H., & Winiger, M. (2002). 1300 years of climatic history for Western Central Asia inferred from tree-rings. *Hoagomia*, 12, 267-277. <https://doi.org/10.1191/0959683602hl543rp>

Harrison, S. P., Yu, G., & Tarasov, P. E. (1996). Late Quaternary lake-level record from northern Eurasia. *Quaternary Research*, 45(2), 138-159. <https://doi.org/10.1006/qres.1996.0016>

Hong, B., Gasse, F., Uchida, M., Hong, Y., Leng, X., Shibata, Y., et al. (2014). Increasing summer rainfall in arid eastern-central Asia over the past 8500 years. *Scientific Reports*, 4, 5279.

Huang, G. W., Chen, J., Zhang, X., Feng, S., & Chen, F. (2015). Definition of the core zone of the "westerlies-dominated climatic regime", and its controlling factors during the instrumental period. *Science China Earth Sciences*, 58(5), 676-684. <https://doi.org/10.1007/s1430-015-0507-y>

Jin, I., Chen, F., Morrill, C., Otto-Bliesner, B. I., & Rasenbloom, N. (2012). Causes of early Holocene desertification in arid central Asia. *Climate Dynamics*, 38(7-8), 1577-1591. <https://doi.org/10.1007/s00382-011-1086-l>

Kaiser, J., Wang, K. J., Rott, D., Li, G., Zheng, Y., Amaral-Zettler, L., et al. (2019). Changes in long chain alkenone distributions and Isochrysidales groups along the Baltic Sea salinity gradient. *Organic Geochemistry*, 127, 92-103. <https://doi.org/10.1016/j.orggeochem.2018.11.012>

Kinnard, C., Zdanowicz, C. M., Fisher, D. A., Isaksson, E., de Vernal, A., & Thompson, I. G. (2011). Reconstructed changes in Arctic sea ice over the past 1,450 years. *Nature*, 479(7374), 509-512. <https://doi.org/10.1038/nature10581>

Lan, J., Xu, H., Sheng, E., Yu, K., Wu, H., Zhou, K., et al. (2018). Climate changes reconstructed from a glacial lake in High Central Asia over the past two millennia. *Quaternary International*, 487, 43-53. <https://doi.org/10.1016/j.quaint.2017.10.035>

Lan, J., Xu, H., Yu, K., Sheng, E., Zhou, K., Wang, T., et al. (2019). Late Holocene hydroclimatic variations and possible forcing mechanisms over the eastern Central Asia. *Science China Earth Sciences*, 62(8), 1288-1301. <https://doi.org/10.1007/s1430-018-9240-x>

Lan, J., Zhang, J., Cheng, P., Ma, X., Ai, L., Chawchai, S., et al. (2020). Late Holocene hydroclimatic variation in central Asia and its response to mid-latitude Westerlies and solar irradiance. *Quaternary Science Reviews*, 238, 106330. <https://doi.org/10.1016/j.quascirev.2020.106330>

Liu, J., Song, X., Sun, X., Yuan, G., Liu, X., & Wang, S. (2009). Isotopic composition of precipitation over arid northwestern China and its implications for the water vapor origin. *Journal of Geographical Sciences*, 19(2), 164-174. <https://doi.org/10.1007/s11430-009-0164-3>

Longo, W. M., Dillon, J. T., Tarozzo, R., Salacup, J. M., & Huang, Y. (2013). Unprecedented separation of long chain alkenones from gas chromatography with a poly(trifluoropropylmethylsiloxane) stationary. *Organic Geochemistry*, 65, 94-102. <https://doi.org/10.1016/j.orggeochem.2013.10.011>

Longo, W. M., Huang, Y., Yao, Y., Zhao, J., Giblin, A. E., Wang, X., et al. (2018). Widespread occurrence of distinct alkenones from Group I haptophytes in freshwater lakes: Implications for paleotemperature and paleoenvironmental reconstructions. *Earth and Planetary Science Letters*, 492, 239-250. <https://doi.org/10.1016/j.epsl.2018.04.002>

Longo, W. M., Theroux, S., Giblin, A. E., Zheng, Y., Dillon, J. T., & Huang, Y. (2016). Temperature calibration and phylogenetically distinct distributions for freshwater alkenones: Evidence from northern Alaskan lakes. *Geochimica et Cosmochimica Acta*, 180, 177-196. <https://doi.org/10.1016/j.gca.2016.02.019>

Luckman, B. H. (2000). The Little Ice Age in the Canadian Rockies. *Geomorphology*, 32(3-4), 357-384. [https://doi.org/10.1016/S0169-555X\(99\)00104-X](https://doi.org/10.1016/S0169-555X(99)00104-X)

Olsen, J., Anderson, N. J., & Knudsen, M. F. (2012). Variability of the North Atlantic Oscillation over the past 5,200 years. *Nature Geoscience*, 5(11), 808-812. <https://doi.org/10.1038/ngeol589>

Pearson, E. J., Juggins, S., & Farrimond, P. (2008). Distribution and significance of long-chain alkenones as salinity and temperature indicators in Spanish saline lake sediments. *Geochimica et Cosmochimica Acta*, 72(16), 4035-4046. <https://doi.org/10.1016/j.gca.2008.05.052>

Pederson, N., Hess, A. E., Baatarbileg, N., Anchukaitis, K. J., & Cosmo, N. D. (2014). Pluvials, droughts, the Mongol Empire, and modern Mongolia. *Proceedings of the National Academy of Sciences*, 111, 43754-379.

Plancq, J., Couto, J. M., Ijaz, U. Z., Leavitt, P. R., & Toney, J. L. (2019). Next-generation sequencing to identify lacustrine haptophytes in the Canadian Prairies: Significance for temperature proxy applications. *Journal of Geophysical Research: Biogeosciences*, 124, 2144-2158. <https://doi.org/10.1029/2018JG004954>

Plancq, J., McColl, J. L., Bendle, J. A., Seki, O., Couto, J. M., Henderson, A. C. G., et al. (2018). Genomic identification of the long-chain alkenone producer in freshwater Lake Toyoni, Japan: Implications for temperature reconstructions. *Organic Geochemistry*, 125, 189-195. <https://doi.org/10.1016/j.orggeochem.2018.09.011>

Putnam, A. E., Putnam, D. E., Andreu-Hayles, L., Cook, E. R., Palmer, J. G., Clark, E. H., et al. (2016). Little Ice Age wetting of interior Asian deserts and the rise of the Mongol Empire. *Quaternary Science Reviews*, 131, 33-50. <https://doi.org/10.1016/j.quascirev.2015.10.033>

Ran, M., & Feng, Z. (2014). Variation in carbon isotopic composition over the past ca. 46,000 yr in the loess-paleosol sequence in central Kazakhstan and paleoclimatic significance. *Organic Geochemistry*, 73, 47-55. <https://doi.org/10.1016/j.orggeochem.2014.05.006>

Richter, N., Longo, W. M., George, S., Shupunova, A., Huang, Y., & Amaral-Zettler, L. (2019). Phylogenetic diversity in freshwater dwelling Isochrysidales haptophytes with implications for alkenone production. *Geobiology*, 17(3), 272-280. <https://doi.org/10.1111/gbi.12330>

Ricketts, R. D., Johnson, T. C., Brown, E. T., Rasmussen, K. A., & Romanovsky, V. V. (2001). The Holocene paleolimnology of Lake Issyk-Kul, Kyrgyzstan: Trace element and stable isotope composition of ostracodes. *Palaeogeography, Palaeoclimatology, Palaeoecology*, 176(1-4), 207-227. [https://doi.org/10.1016/S0031-0182\(01\)0339-X](https://doi.org/10.1016/S0031-0182(01)0339-X)

Rudaya, N., Tarasov, P., Dorofeyuk, N., Solovieva, N., Kalugin, I., Andreev, A., et al. (2009). Holocene environments and climate in the Mongolian Altai reconstructed from the Hoton-Nur pollen and diatom records: A step towards better understanding climate dynamics in Central Asia. *Quaternary Science Reviews*, 28(5-6), 540-554. <https://doi.org/10.1016/j.quascirev.2008.10.013>

Shi, Y., Shen, Y., Kang, E., Li, D., Ding, Y., Zhang, G., & Hu, R. (2007). Recent and future climate change in northwest China. *Climatic Change*, 80(3-4), 379-393. <https://doi.org/10.1007/s10584-006-9121-7>

Sinha, A., Berkelhammer, M., Slot, L., Mudelsee, M., Cheng, H., & Biswas, J. (2011). The leading mode of Indian Summer Monsoon precipitation variability during the last millennium. *Geophysical Research Letters*, 38, L15703. <https://doi.org/10.1029/2011GL047713>

Song, M., Zhou, A., He, Y., Zhao, C., Wu, J., Zhao, Y., et al. (2016). Environmental controls on long-chain alkenone occurrence and compositional patterns in lacustrine sediments, northwestern China. *Organic Geochemistry*, 91, 43-53. <https://doi.org/10.1016/j.orggeochem.2015.10.009>

Theroux, S., D'Andrea, W. J., Toney, J., Amaral-Zettler, L., & Huang, Y. (2010). Phylogenetic diversity and evolutionary relatedness of alkenone-producing haptophyte algae in lakes: Implications for continental paleotemperature reconstructions. *Earth and Planetary Science Letters*, 300(3-4), 311-320. <https://doi.org/10.1016/j.epsl.2010.10.009>

Trabucco, A., & Zomer, R. J. (2009). Global Aridity Index (Global-Aridity) and Global Potential Evapo-Transpiration (Global-PET) Geospatial Database. CGIAR Consortium for Spatial Information. Published online, available from the CGIAR-CSIGeoPortal at <http://www.cgiar.org>

Trouet, V., Esper, J., Graham, N. E., Baker, A., Scourse, J. D., & Frank, D. C. (2009). Persistent positive North Atlantic Oscillation mode dominated the Medieval Climate Anomaly. *Science*, 324(5923), 78-80. <https://doi.org/10.1126/science.1166349>

Wang, K. J., O'Donnell, J. A., Longo, W. M., Amaral-Zettler, L., Li, G., Yao, Y., & Huang, Y. (2019). Group I alkenones and Isochrysidales in the world's largest maar lakes and their potential paleoclimate applications. *Organic Geochemistry*, 138, 103924. <https://doi.org/10.1016/j.orggeochem.2019.103924>

Wang, L., Longo, W. M., Dillon, J. T., Zhao, J., Zheng, Y., Moros, M., & Huang, Y. (2019). An efficient approach to eliminate sterol ethers and miscellaneous esters/ketones for gas chromatographic analysis for alkenones and alkenoates. *Journal of Chromatography A*, 1596, 175-182. <https://doi.org/10.1016/j.chroma.2019.02.064>

Wang, S., & Dou, H. (1998). *China Lake Record (in Chinese)* (pp. 348-349). Beijing: Science Press.

Wang, S., Zhang, M., Crawford, J., Hughes, C. E., Du, M., & Liu, X. (2017). The effect of moisture source and synoptic conditions on precipitation isotopes in arid central Asia. *Journal of Geophysical Research: Atmospheres*, 122, 2667-2682. <https://doi.org/10.1002/2015JD024626>

Wang, W., & Feng, Z. (2013). Holocene moisture evolution across the Mongolian Plateau and its surrounding areas: A synthesis of climatic records. *Earth-Science Reviews*, 122, 38-57. <https://doi.org/10.1016/j.earscirev.2013.03.005>

Xie, H., Zhang, H., Ma, J., Li, G., Wang, Q., Rao, Z., et al. (2018). Trend of increasing Holocene summer precipitation in arid central Asia: Evidence from an organic carbon isotopic record from the LJW10 loess section in Xinjiang, NW China. *Palaeogeography, Palaeoclimatology, Palaeoecology*, 509, 24-32. <https://doi.org/10.1016/j.palaeo.2018.04.006>

Xu, H., Zhou, K., Lan, J., Zhang, G., & Zhou, X. (2019). Arid Central Asia saw mid-Holocene drought. *Geology*, 47, 255-258. <https://doi.org/10.1130/G45686.1>

Yao, J., Chen, Y., Zhao, Y., Guan, X., Mao, W., & Yang, L. (2020). Climatic and associated atmospheric water cycle change over the Xinjiang, China. *Journal of Hydrology*, 585, 124823. <https://doi.org/10.1016/j.jhydrol2020.124823>

Yao, T., Thompson, L.G., Qin, D., Tian, L., Jiao, K., Yang, Z., et al. (1996). Variations in temperature and precipitation in the past 2000 a on the Xizang (Tibet) Plateau-Guliyai ice core record. *Science in China Series D: Earth Sciences*, 39, 425-433.

Yao, Y., Zhao, J., Longo, W. M., Li, G., Wang, X., Vachula, R.S., et al. (2019). New insights into environmental controls on the occurrence and abundance of Group I alkenones and their paleoclimate applications: Evidence from volcanic lakes of northeastern China. *Earth and Planetary Science Letters*, 527, 115792. <https://doi.org/10.1016/j.epsl.2019.115792>

Zhang, P., Cheng, H., Edwards, R. L., Chen, F., Wang, Y., Yang, X., et al. (2008). A test of climate, sun, and culture relationships from an 1810-year Chinese cave record. *Science*, 322(5903), 940-942. <https://doi.org/10.1126/science.1163965>

Zhao, Y., Liu, H., Zhang, A., Gui, X., & Zhao, A. (2019). Spatiotemporal variations and its influencing factors of grassland net primary productivity in Inner Mongolia, China during the period 2000-2014. *Journal of Arid Environments*, 165, 106-115. <https://doi.org/10.1016/j.jaridenv.2019.01.004>

Zheng, Y., Heng, P., Conte, M. H., Vachula, R. S., & Huang, Y. (2019). Systematic chemotaxonomic profiling and novel paleotemperature indices based on alkenones and alkenoates: Potential for disentangling mixed species input. *Organic Geochemistry*, 128, 26-41. <https://doi.org/10.1016/j.orggeochem.2018.12.008>

Zheng, Y., Tarozo, R., & Huang, Y. (2017). Optimizing chromatographic resolution for simultaneous quantification of long chain alkenones, alkenoates and their double bond positional isomers. *Organic Geochemistry*, 111, 136-143. <https://doi.org/10.1016/j.orggeochem2017.06.013>